

Bidirectional DC - DC Converter Topology for Electric Vehicles Using Fuzzy Logic Controller

Shaik Daryabi¹ R.Chandra Sekha² B.Nagendra³ G.Surya Sai Ganesh⁴ A.Kamalesh Benny⁵

Asst.Professor, Department of EEE, Raghu Engg. College, Visakhapatnam, AP, India.¹

B.Tech Students, Department of EEE, Raghu Engg. College, Visakhapatnam, AP, India.^{2,3,4,5}

ABSTRACT: This project organizes an application of hybrid electric vehicle systems operated with novel designed bidirectional dc-dc converter (BDC) which interfaces a main energy storage (ES1), an auxiliary energy storage (ES2) and dc bus of different voltage levels. Proposed BDC converter can operate both step up and step-down mode. In which step up mode represents low voltage dual source -powering mode and step-down mode represents high voltage dc link energy –regenerating mode, both the modes are operated under the control of bidirectional power flow. This model can independently control power flow between low voltage dual source buck/boost modes. Here in, the circuit configuration, operation, steady-state analysis, and closed-loop control of the proposed BDC are discussed according to its three modes of power transfer. In this project fuzzy logic controller is used and also system results are validating through MATLAB/SIMULINK software.

Index Terms—Bidirectional dc/dc converter (BDC), dual battery storage, hybrid electric vehicle, Fuzzy logic controller.

I. INTRODUCTION

Worldwide environmental change and energy supply is declining have stimulated changes in vehicular innovation. For the applications in future vehicles the advanced technologies are currently being investigated. Among such applications, fuel-cell hybrid electric vehicles (FCV/HEV) are efficient

and promising candidates. Before, Ehsani et al. studied the vehicles' dynamics to look for an optimal torque-speed profile of the electric propulsion system. Emadi et al. talked about the working properties of the geographies for various vehicles including HEV, FCV, and more electric vehicles. To satisfy huge vehicular load, for advanced vehicular power system Emadi et al. also integrated power electronics intensive solutions. Schaltz et al. sufficiently divide the load power among the fuel cell stack, the battery, and the ultra-capacitors based on two proposed energy-management strategies. Thounthong et al. studied the impact of fuel-cell (FC) execution and the benefits of hybridization for control systems. Chan et al. reviewed electric, hybrid, and fuel-cell vehicles and concentrated on structures and modeling for energy management. Khaligh and Li introduced energy-storage topologies for HEVs and plug-in HEVs (PHEVs). They also analyzed and compared battery, UC, and FC technologies. Moreover, they also addressed various hybrid ESSs that integrate two or more storage devices. Rajasekar talked about the flow status and the necessities of essential electric drive parts—the battery, the electric motors, and the power electronics system. Lai et al. implemented a bidirectional dc/dc converter topology with two-stage and interleaved qualities.

The Voltage Transformation ratio of the converter has improved in the EV and DC micro grid systems. In addition, Lai likewise examined a BDC topology which has a high voltage conversion ratio for EV batteries associated with a dc-micro grid system. In fuel-cell hybrid electricvehicle systems, the primary battery storage device is commonly used to begin the FC and to supply power to the propulsion motor.

The battery storage devices improve the inherently slowresponse time for the FC stack through supplying peak power during accelerating the vehicle. Besides, it contains a high power-density component for example, supercapacitors(SCs) eliminate peak power transients during accelerating and regenerative braking. In general, SCs can store regenerative energy during deceleration and release it during acceleration, thereby supplying additional power. The high-power density of super capacitor extends the life span of both FC stack and battery storage devices and improves the overall efficiency of FCV systems.

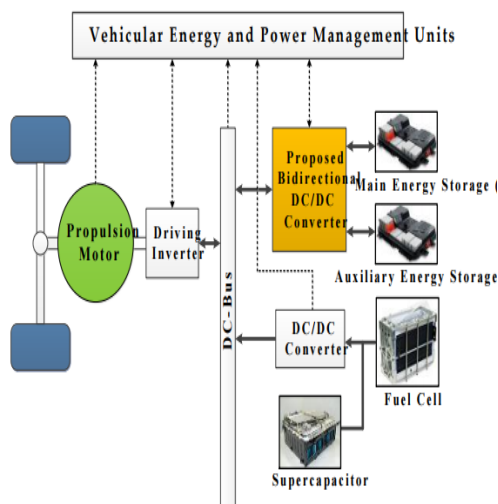


Fig.1. Typical functional diagram for a FCV/HEV power system.

This investigation proposes an interleaved voltage-doublers structure and a synchronous buck-boost circuit are a two new BDC topologies for FCV/HEV power system. It highlights two essential working modes: a low-voltage double-source-powering mode and a high-voltage dc-bus energy-regenerating mode. In addition, when the converter is in low-voltage dual-source buck-boost mode the proposed converter can independently control power flow between any two low-voltage sources. A similar topology was presented in that just discuss a short idea. On the other hand, this investigation presents detailed analysis of the operation and closed-loop control of this new topology as well as simulation results for all its modes of operation. The proposed converter can operate over a wider range of voltage levels that's why this study expanded the topology presented in.

The principle attributes of the proposed converter are summed up as follows:

- Interfaces more than two dc sources for various voltage levels,
- Controls power flow between the dc bus and the two low-voltage sources and furthermore independently controls power flow between the two low-voltage sources,
- Enhances static voltage gain and therefore decreases switch voltage stress, and
- Possesses a sensible duty cycle and makes a wide voltage distinction between its high- and low-side ports.

II. PROPOSED TOPOLOGY

The proposed BDC topology with dual-battery energy storage is illustrated in Fig.2.1, where VH, VES1, and VES2 represent the high-

voltage dc-bus voltage, the main energy storage (ES1), and the auxiliary energy storage (ES2) of the system, individually. To turn ON or turn OFF the current loops of ES1 and ES2, the two bidirectional power switches (SES1 and SES2) in the converter structure, are utilized. A charge-pump capacitor (CB) is incorporated as a voltage divider. The voltage divider consists of the four active switches (Q1, Q2, Q3, Q4) and two-phase inductors (L1, L2) to improve the static voltage gain in the middle of the two high-voltage dc bus (VH) and low-voltage dual sources (VES1, VES2) in the proposed converter. Moreover, the extra CB decreases the switch voltage stress of active switches and eliminates the need to operate at an extreme duty ratio. Furthermore, the three bidirectional power switches (S, SES1, SES2) showed in Fig. 4.2 display four-quadrant operation and are adopted to control the power flow between two low-voltage dual sources (VES1, VES2) and to block either positive or negative voltage.

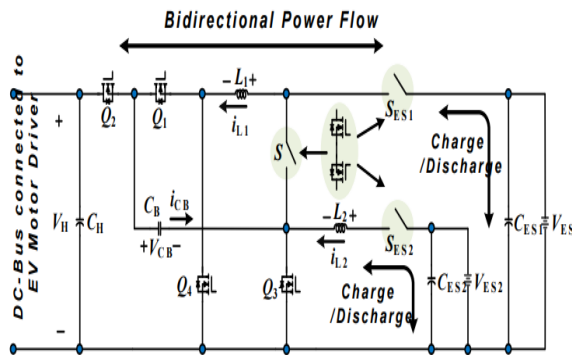


Fig.2.1. Proposed BDC topology with dual-battery energy storage.

This bidirectional power switch is implemented via two metal-oxide-semiconductor field-effect transistors (MOSFETs), pointing in opposite directions, in series connection. To explain the concept for the proposed converter, all the conduction statuses of the power devices

involved in each operation mode are displayed in Table 2.1. Accordingly, the four operating modes are illustrated as follows to enhance understanding.

TABLE 2.1.
CONDUCTION STATUS OF DEVICES FOR DIFFERENT OPERATING MODES

Operating Modes	ON	OFF	Control Switch	Synchronous Rectifier (SR)
Low-voltage dual-source-powering mode (Accelerating, $x_1=1, x_2=1$)	S_{ES1}, S_{ES2}	S	Q_3, Q_4	Q_1, Q_2
High-voltage dc-bus energy-regenerating mode (Braking, $x_1=1, x_2=1$)	S_{ES1}, S_{ES2}	S	Q_1, Q_2	Q_3, Q_4
Low-voltage dual-source buck mode (ES1 to ES2, $x_1=0, x_2=0$)	S_{ES1}, S_{ES2}	Q_1, Q_3, Q_4	S	Q_2
Low-voltage dual-source boost mode (ES2 to ES1, $x_1=0, x_2=0$)	S_{ES1}, S_{ES2}	Q_1, Q_3, Q_4	Q_2	S
System shutdown	-	S_{ES1}, S_{ES2} Q_1, Q_3, Q_4	-	-

2.1. Low-Voltage Dual-Source-Powering Mode

Fig. 2.2 shows the circuit schematic and steady-state waveforms for the converter under the low-voltage dual-source-powering mode. Where, the switch S is OFF, and S_{ES1}, S_{ES2} are ON, and the two low-voltage double sources (VES1, VES2) are delivering the energy to the dc-bus and loads. The high-side switches $Q1$ and $Q2$ operates as the synchronous rectifier (SR) and the low-side switches $Q3$ and $Q4$ are actively switching at a phase-shift angle of 180° in this mode. Based on the typical waveforms shown in Fig.2.2 (b), when the duty ratio is larger than 50%, hence the four circuit states are possible as found in Fig. 2.3. The working principle of the BDC in low-voltage double-source-powering mode and the on/off status of the active switches, the working can be justified short note as.

1) State 1 [$t_0 < t < t_1$]: In this state, the switches $Q1, Q3$ are switched ON, and $Q2, Q4$ are switched OFF, the time interval is $(1-D_u)T_{sw}$. The i_{L1} decreases linearly from the initial value because the voltage across $L1$ is the difference between the low-side voltage V_{ES1} and the

charge-pump voltage (VCB). In addition, the energy source VES2 is utilized to charge inductor L2,

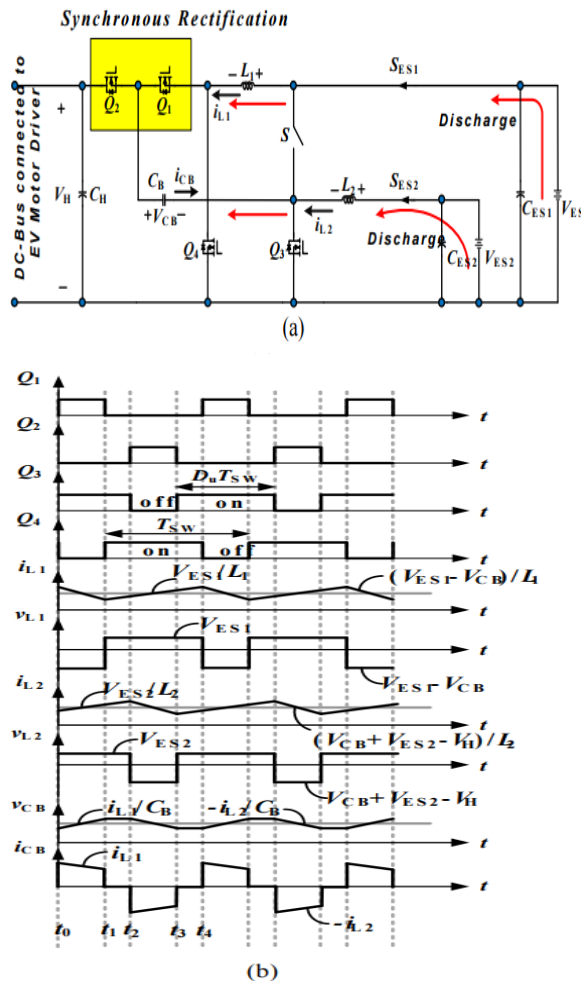


Fig. 2.2. Low-voltage dual-source-powering mode of the proposed BDC: (a) circuit schematic and (b) steady-state waveforms. thereby generating a linear increase in the inductor current. The voltages across inductors L1 and L2 can be denoted as

$$L_1 \frac{di_{L1}}{dt} = V_{ES2} - V_{CB} \quad (1)$$

$$L_2 \frac{di_{L2}}{dt} = V_{ES2} \quad (2)$$

State 2 [$t_1 < t < t_2$]: During this state, the interval time is $(D_s - 0.5)T_{sw}$; switches Q3 and Q4 are turned on; and switches Q1 and Q2 are turned

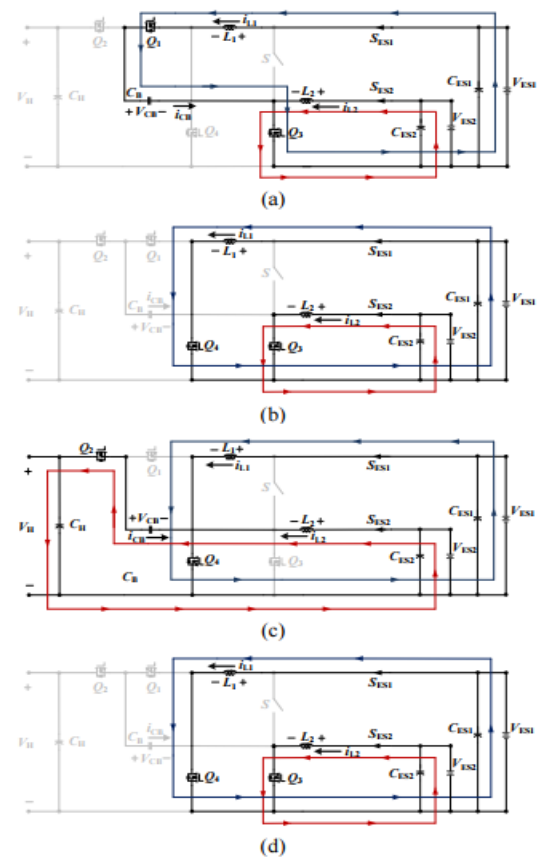


Fig. 2.3 Circuit states of the proposed BDC for the low-voltage dual-source-powering mode. (a) State 1. (b) State 2. (c) State 3. (d) State 4.

a) off. The low-side voltages VES1 and VES2 are located between inductors L1 and L2, respectively, thereby linearly increasing the inductor currents, and initiating energy to storage. The voltages across inductors L1 and L2 under state 2 can be denoted as

$$L_1 \frac{di_{L1}}{dt} = V_{ES1} \quad (3)$$

$$L_2 \frac{di_{L2}}{dt} = V_{ES2} \quad (4)$$

- b) State 3 [$t_2 < t < t_3$]: During this state, the interval time is $(1-D_u)T_{sw}$; switches Q1 and Q3 are turned on, whereas switches Q2 and Q4 are turned off. The voltages across inductors L1 and L2 can be denoted as

$$L_1 \frac{di_{L1}}{dt} = V_{ES1} \quad (5)$$

$$L_2 \frac{di_{L2}}{dt} = V_{CB} + V_{ES2} - V_H \quad (6)$$

- c) State 4 [$t_3 < t < t_4$]: During this state, the interval time is $(D_u - 0.5)T_{sw}$; switches Q3 and Q4 are turned on, and switches Q1 and Q2 are turned off. The voltages across inductors L1 and L2 can be denoted as

$$L_1 \frac{di_{L1}}{dt} = V_{ES1}$$

$$L_2 \frac{di_{L2}}{dt} = V_{ES2}$$

2.2. High-Voltage DC-Bus Energy-Regenerating Mode :

In the High-Voltage DC-Bus Energy-Regenerating mode, during regenerative braking operation, the kinetic energy stored in the motor drive is fed back to the source. The absorbed power of the battery is lower than the regenerative power. Consequently, the excess energy is utilized to charge the energy storage device. The high-voltage dc bus energy-regenerating mode circuit diagram and the

steady-state waveforms of the BDC are found in Fig.4.4.

In that, the switches Q1 and Q2 are utilized to control the current in the inductors, which have a phase-shift angle of 180° . The current in the inductor directly flows away from the dc-bus and toward the dual energy storage devices. To improve the conversion efficiency, the switches Q3 and Q4 work as the SR. Based on the steady-state waveforms appeared in Fig. 4.4(b), when the duty ratio is below 50%, four different circuit states are possible, as found in Fig. 4.5. The operating principle and the ON-OFF status of the switches of the BDC in high-voltage dc-bus energy-regenerating mode, the operation can be explained briefly as follows.

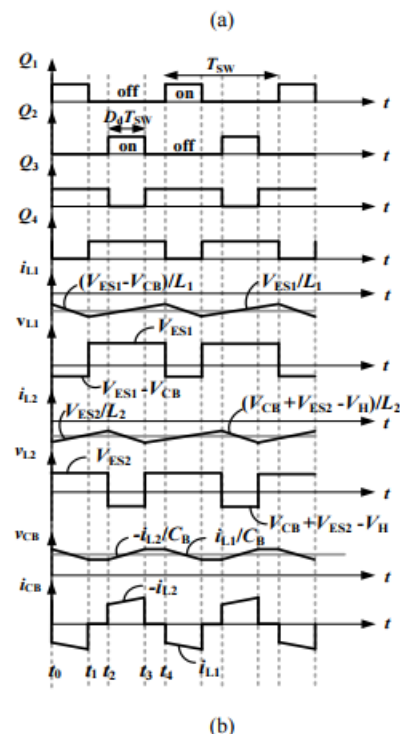
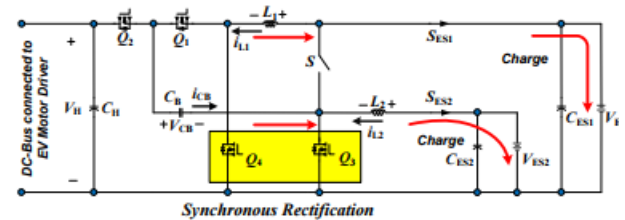
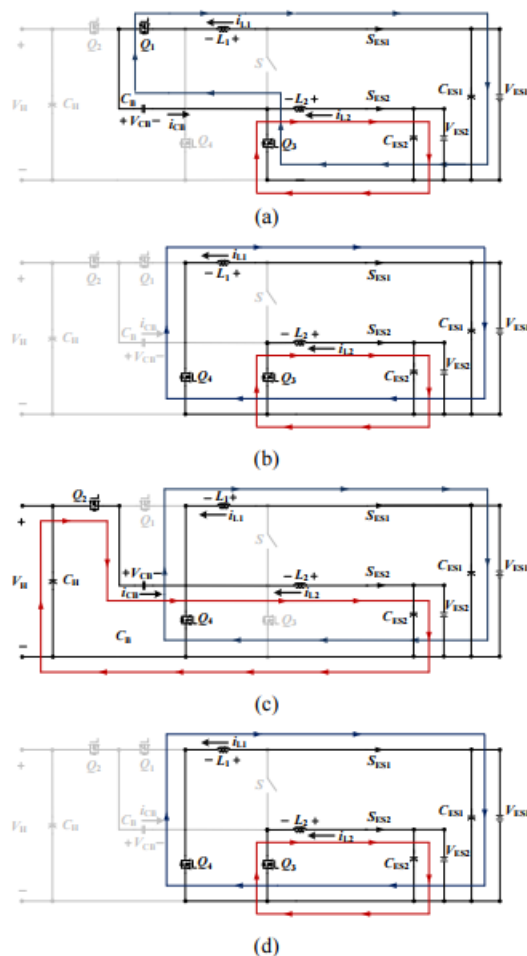


Fig.2.4. High-voltage dc-bus energy-regenerating mode of the proposed BDC: (a) circuit schematic and (b) steady-state waveforms.

On the basis of the steady-state waveforms shown in Fig. 2.4(b), when the duty ratio is below 50%, four different circuit states are possible, as shown in Fig. 2.5. In the light of the on-off status of the active switches and the operating principle of the BDC in high-voltage dc-bus energy-regenerating mode, the operation can be depicted briefly as follows.



denoted as

$$L_1 \frac{di_{L1}}{dt} = V_{ES1} \quad (13)$$

$$L_2 \frac{di_{L2}}{dt} = V_{ES2} + V_{CB} - V_H \quad (14)$$

d) State 4 [$t_3 < t < t_4$]: During this state, the interval time is $(0.5-D_d)T_{sw}$; switches Q3 and Q4 are turned on, and switches Q1 and Q2 are turned off. The voltages across inductors L1 and L2 can be denoted as

$$L_1 \frac{di_{L1}}{dt} = V_{ES1} \quad (15)$$

$$L_2 \frac{di_{L2}}{dt} = V_{ES2} \quad (16)$$

Remaining modes of operation were explained in [1].

3. FUZZY CONTROLLER:

The word Fuzzy means vagueness. Fuzziness occurs when the boundary of piece of information is not clear-cut. In 1965 Lotfi A. Zahed propounded the fuzzy set theory. Fuzzy set theory exhibits immense potential for effective solving of the uncertainty in the problem. Fuzzy set theory is an excellent mathematical tool to handle the uncertainty arising due to vagueness. Understanding human speech and recognizing handwritten characters are some common instances where fuzziness manifests.

Fuzzy set theory is an extension of classical set theory where elements have varying degrees of membership. Fuzzy logic uses the whole interval between 0 and 1 to describe human reasoning. In FLC the input variables are mapped by sets of membership functions and these are called as “FUZZY SETS”.

Fuzzy set comprises from a membership function which could be defines by parameters. The value between 0 and 1 reveals a degree of

membership to the fuzzy set. The process of converting the crisp input to a fuzzy value is called as “fuzzification.” The output of the Fuzzier module is interfaced with the rules. The basic operation of FLC is constructed from fuzzy control rules utilizing the values of fuzzy sets in general for the error and the change of error and control action. Basic fuzzy module is shown in fig.5

The results are combined to give a crisp output controlling the output variable and this process is called as “DEFUZZIFICATION.”

4.1 MATLAB CIRCUITS:

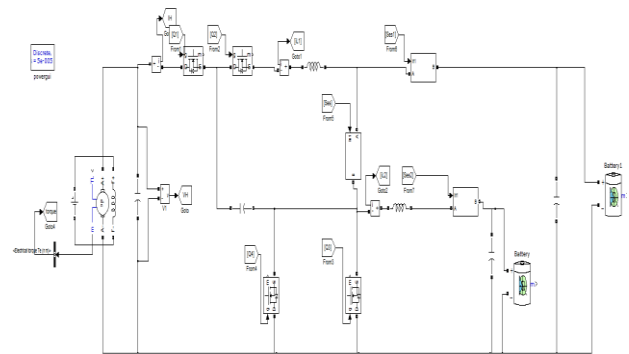


Fig4.1 Simulation Block Diagram

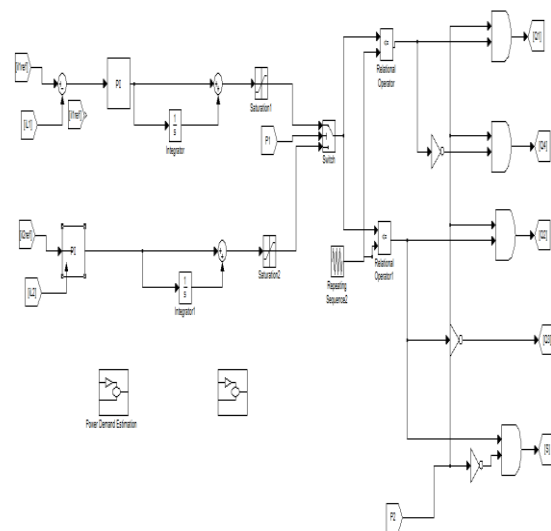


Fig4.2 Simulation Control Diagram

4.2 WAVE FORMS:

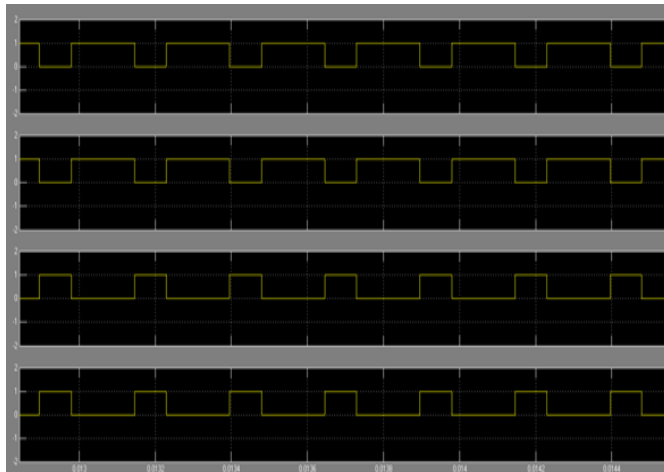
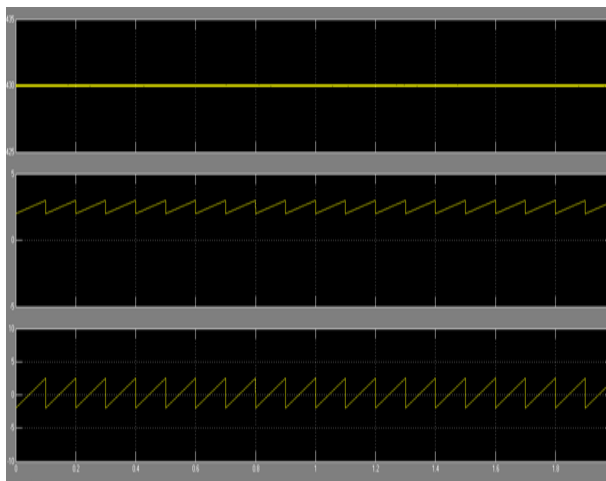


Fig. 4.3. Measured waveforms for low-voltage dual-source-powering mode:(a) gate signals



(b) output voltage and inductor currents.

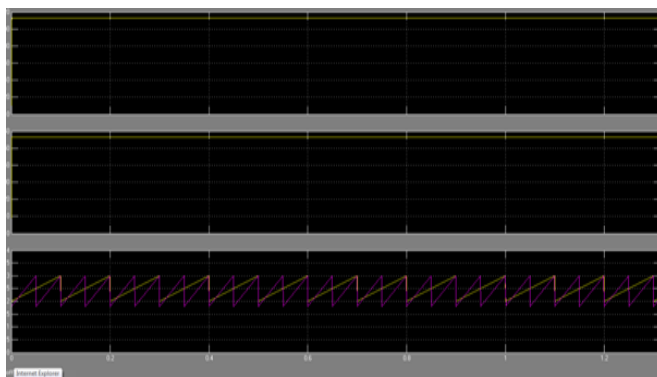


Fig. 4.4. Measured waveforms for high-voltage dc-bus energy-regenerating mode:.

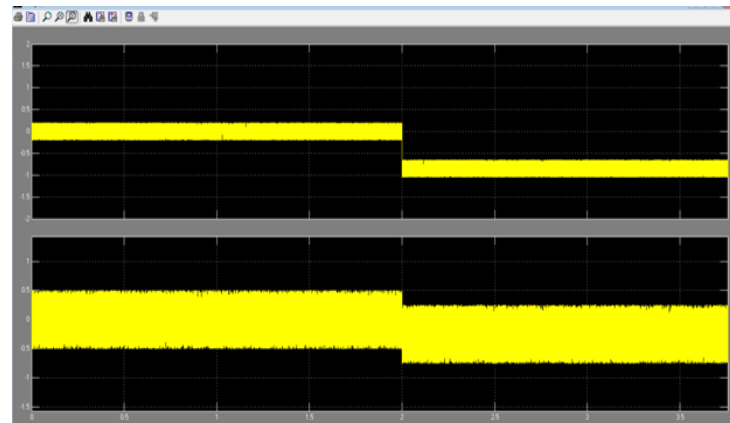


Fig.4.5. Waveforms of controlled current step change in the low-voltage dual-source-powering mode by simulation

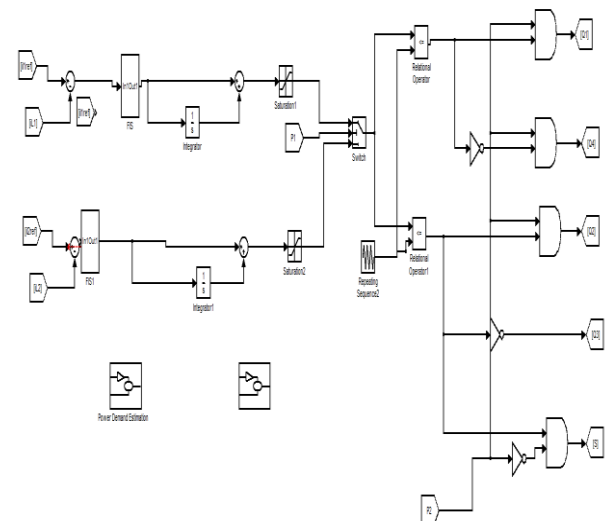


Fig4.6 Simulation of fuzzy logic Control Diagram

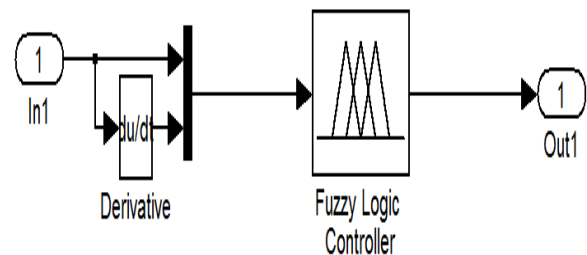


Fig4.7 fuzzy logic Controller

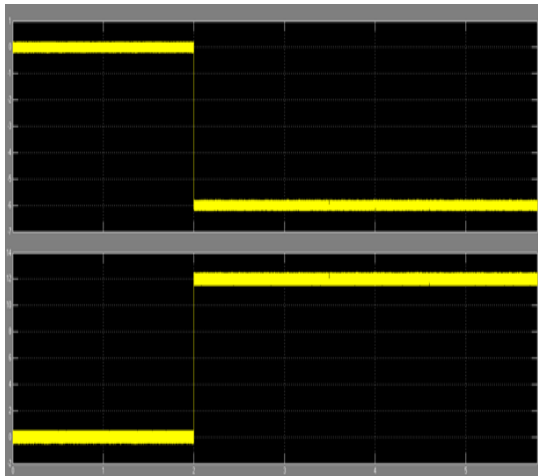


Fig. 4.8 Waveforms of controlled current step change in the low-voltage dual-source boost mode: by simulation;

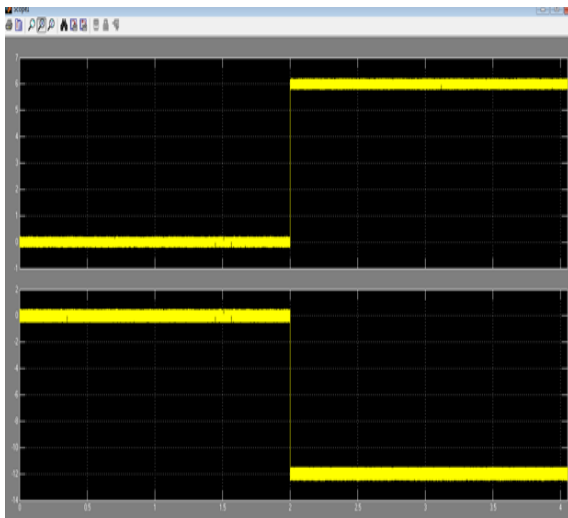


Fig. 4.9 Waveforms of controlled current step change in the low-voltage dual-source buck mode: by simulation

CONCLUSION

A new BDC topology was introduced to interface dual battery energy sources and high-voltage dc bus of various voltage levels. The circuit design, operation principles, analyses, and static voltage gains of the proposed BDC were talked about based on various methods of power transfer. Simulation waveforms for a 1 kW sample system featured the presentation and possibility of this suggested BDC topology. The

highest transformation efficiencies were 97.25%, 95.32%, 95.76%, and 92.67% for the high-voltage dc-bus energy-regenerative buck mode, low-voltage double-source-powering mode, low-voltage double-source boost mode (ES2 to ES1), and low-voltage dual-source buck mode (ES1 to ES2), individually. The results exhibit that the proposed BDC can be effectively applied in FC/HEV systems to produce hybrid power architecture.

REFERENCES

- [1] M. Ehsani, K.M. Rahman, and H.A. Toliyat, "Propulsion system design of electric and hybrid vehicles," *IEEE Transactions on industrial electronics*, vol. 44, no.1, pp. 19-27, 1997.
- [2] A. Emadi, K. Rajasekar, S.S. Williamson, and S.M. Lukic, "Topological overview of hybrid electric and FCV power system architectures and configurations," *IEEE Transactions on Vehicular Technology*, vol. 54, no. 3, pp. 763-770, 2005.
- [3] A. Emadi, S.S. Williamson, and A. Khaligh, "Power electronics intensive solutions for advanced electric, hybrid electric, and fuel cell vehicular power systems," *IEEE Transactions on Power Electronics*, vol. 21, no. 3, pp. 567-577, 2006.
- [4] E. Schaltz, A. Khaligh, and P.O. Rasmussen, "Influence of battery/ultracapacitor energy-storage sizing on battery lifetime in a fuel cell hybrid electric vehicle," *IEEE Transactions on Vehicular Technology*, vol. 58, no. 8, pp. 3882-3891, 2009.
- [5] P. Thounthong, V. Chunkag, P. Sethakul, B. Davat, and M. Hinaje, "Comparative study of fuel-cell vehicle hybridization with battery or supercapacitor storage device," *IEEE transactions on vehicular technology*, vol. 58, no. 8, pp. 3892-3904, 2009.
- [6] C.C. Chan, A. Bouscayrol, and K. Chen, "Electric, hybrid, and fuel-cell vehicles: Architectures and modeling," *IEEE transactions on vehicular technology*, vol. 59, no. 2, pp. 589-598, 2010.
- [7] A. Khaligh and Z. Li, "Battery, ultra capacitor, FC, and hybrid energy storage systems for electric, hybrid electric, fuel cell, and plug-in hybrid electric vehicles: State of the art," *IEEE transactions on Vehicular Technology*, vol. 59, no. 6, pp. 2806-2814, 2010.

[8] K.Rajashekara,"Present status and future trends in electric vehiclepropulsion technologies," IEEE Journal of Emerging and Selected Topics in PowerElectronics, vol. 1, no. 1, pp. 3-10, 2013.

[9] C.-M.Lai,Y.-C.Lin,andD.Lee,"Study and implementation of a two-phase interleaved bidirectional DC/DC converter for vehicle and dc-microgrid systems," Energies, vol. 8, no. 9, pp. 9969-991, 2015.

[10] C.-M.Lai,"Development of a novel bidirectional DC/DC converter topology with high voltage conversion ratio for electricvehicles and DC-micro grids," Energies, vol. 9, no. 6, p. 410, 2016.